Transverse-Mass Dependence of Two-Pion Correlations in Au + Au Collisions at $\sqrt{s_{NN}} = 130$ GeV

K. Adcox,[40] S. S. Adler,[3] N. N. Ajitanand,[27] Y. Akiba,[14] J. Alexander,[27] L. Aphecetche,[34] Y. Arai,[14] S. H. Aronson,[3] R. Averbeck,[28] T. C. Awes,[29] K. N. Barish,[5] P. D. Barnes,[19] J. Barrette,[21] B. Bassalleck,[25] S. Bathe,[22] V. Baublis,[30] A. Bazilevsky,[12,32] S. Belikov,[12,13] F. G. Bellaiche,[29] S. T. Belyaev,[16] M. J. Bennett,[19] Y. Berdnikov,[35] S. Botelho,[33] M. L. Brooks,[19] D. S. Brown,[26] N. Bruner,[25] D. Bucher,[22] H. Buesching,[22] V. Bumazhnov,[12] G. Bunce,[3,32] J. Burward-Hoy,[28] S. Butsyk,[28,30] T. A. Carey,[19] P. Chand,[2] J. Chang,[5] W. C. Chang,[1] L. L. Chavez,[25] S. Chernichenko,[12] C. Y. Chi,[8] J. Chiba,[14] M. Chiu,[8] R. K. Choudhury,[2] T. Christ,[28] T. Chujo,[3,39] M. S. Chung,[15,19] P. Chung,[27] V. Cianciolo,[29] B. A. Cole,[8] D. G. D'Enterria,[34] G. David,[3] H. Delagrange,[34] A. Denisov,[12] A. Deshpande,[32] E. J. Desmond,[3] O. Dietzsch,[33] B. V. Dinesh,[2] A. Drees,[28] A. Durum,[12] D. Dutta,[2] K. Ebisu,[24] Y. V. Efremenko,[29] K. El Chenawi,[40] A. Enokizono,[11] H. En'yo,[17,31] S. Esumi,[39] L. Ewell,[3] T. Ferdousi,[5] D. E. Fields,[25] S. L. Fokin,[16] Z. Fraenkel,[42] A. Franz,[3] A. D. Frawley,[9] S.-Y. Fung,[5] S. Garpman,[20,*] T. K. Ghosh,[40] A. Glenn,[36] A. L. Godoi,[33] Y. Goto,[32] S. V. Greene,[40] M. Grosse Perdekamp,[32] S. K. Gupta,[2] W. Guryn,[3] H.-Å Gustafsson,[20] J. S. Haggerty,[3] H. Hamagaki,[7] A. G. Hansen,[19] H. Hara,[24] E. P. Hartouni,[18] R. Hayano,[38] N. Hayashi,[31] X. He,[10] T. K. Hemmick,[28] J. M. Heuser,[28] M. Hibino,[41] J. C. Hill,[13] D. S. Ho,[43] K. Homma,[11] B. Hong,[15] A. Hoover,[26] T. Ichihara,[31,32] K. Imai,[17,31] M. S. Ippolitov,[16] M. Ishihara,[31,32] B. V. Jacak,[28,32] W. Y. Jang,[15] J. Jia,[28] B. M. Johnson,[3] S. C. Johnson,[18,28] K. S. Joo,[23] S. Kametani,[41] J. H. Kang,[43] M. Kann,[30] S. S. Kapoor,[2] S. Kelly,[8] B. Khachaturov,[42] A. Khanzadeev,[30] J. Kikuchi,[41] D. J. Kim,[43] H. J. Kim,[43] S. Y. Kim,[43] Y. G. Kim,[43] W. W. Kinnison,[19] E. Kistenev,[3] A. Kiyomichi,[39] C. Klein-Boesing,[22] S. Klinksiek,[25] L. Kochenda,[30] V. Kochetkov,[12] D. Koehler,[25] T. Kohama,[11] D. Kotchetkov,[5] A. Kozlov,[42] P. J. Kroon,[3] K. Kurita,[31,32] M. J. Kweon,[15] Y. Kwon,[43] G. S. Kyle,[26] R. Lacey,[27] J. G. Lajoie,[13] J. Lauret,[27] A. Lebedev,[13,16] D. M. Lee,[19] M. J. Leitch,[19] X. H. Li,[5] Z. Li,[6,31] D. J. Lim,[43] M. X. Liu,[19] X. Liu,[6] Z. Liu,[6] C. F. Maguire,[40] J. Mahon,[3] Y. I. Makdisi,[3] V. I. Manko,[16] Y. Mao,[6,31] S. K. Mark,[21] S. Markacs,[8] G. Martinez,[34] M. D. Marx,[28] A. Masaike,[17] F. Matathias,[28] T. Matsumoto,[7,41] P. L. McGaughey,[19] E. Melnikov,[12] M. Merschmeyer,[22] F. Messer,[28] M. Messer,[3] Y. Miake,[39] T. E. Miller,[40] A. Milov,[42] S. Mioduszewski,[3,36] R. E. Mischke,[19] G. C. Mishra,[10] J. T. Mitchell,[3] A. K. Mohanty,[2] D. P. Morrison,[3] J. M. Moss,[19] F. Mühlbacher,[28] M. Muniruzzaman,[5] J. Murata,[31] S. Nagamiya,[14] Y. Nagasaka,[24] J. L. Nagle,[8] Y. Nakada,[17] B. K. Nandi,[5] J. Newby,[36] L. Nikkinen,[21] P. Nilsson,[20] S. Nishimura,[7] A. S. Nyanin,[16] J. Nystrand,[20] E. O'Brien,[3] C. A. Ogilvie,[13] H. Ohnishi,[3,11] I. D. Ojha,[4,40] M. Ono,[39] V. Onuchin,[12] A. Oskarsson,[20] L. Österman,[20] I. Otterlund,[20] K. Oyama,[7,38] L. Paffrath,[3,*] A. P. T. Palounek,[19] V. S. Pantuev,[28] V. Papavassiliou,[26] S. F. Pate,[26] T. Peitzmann,[22] A. N. Petridis,[13] C. Pinkenburg,[3,27] R. P. Pisani,[3] P. Pitukhin,[12] F. Plasil,[29] M. Pollack,[28,36] K. Pope,[36] M. L. Purschke,[3] I. Ravinovich,[42] K. F. Read,[29,36] K. Reygers,[22] V. Riabov,[30,35] Y. Riabov,[30] M. Rosati,[13] A. A. Rose,[40] S. S. Ryu,[43] N. Saito,[31,32] A. Sakaguchi,[11] T. Sakaguchi,[7,41] H. Sako,[39] T. Sakuma,[31,37] V. Samsonov,[30] T. C. Sangster,[18] R. Santo,[22] H. D. Sato,[17,31] S. Sato,[39] S. Sawada,[14] B. R. Schlei,[19] Y. Schutz,[34] V. Semenov,[12] R. Seto,[5] T. K. Shea,[3] I. Shein,[12] T.-A. Shibata,[31,37] K. Shigaki,[14] T. Shiina,[19] Y. H. Shin,[43] I. G. Sibiriak,[16] D. Silvermyr,[20] K. S. Sim,[15] J. Simon-Gillo,[19] C. P. Singh,[4] V. Singh,[4] M. Sivertz,[3] A. Soldatov,[12] R. A. Soltz,[18] S. Sorensen,[29,36] P. W. Stankus,[29] N. Starinsky,[21] P. Steinberg,[8] E. Stenlund,[20] A. Ster,[44] S. P. Stoll,[3] M. Sugioka,[31,37] T. Sugitate,[11] J. P. Sullivan,[19] Y. Sumi,[11] Z. Sun,[6] M. Suzuki,[39] E. M. Takagui,[33] A. Taketani,[31] M. Tamai,[41] K. H. Tanaka,[14] Y. Tanaka,[24] E. Taniguchi,[31,37] M. J. Tannenbaum,[3] J. Thomas,[28] J. H. Thomas,[18] T. L. Thomas,[25] W. Tian,[6,36] J. Tojo,[17,31] H. Torii,[17,31] R. S. Towell,[19] I. Tserruya,[42] H. Tsuruoka,[39] A. A. Tsvetkov,[16] S. K. Tuli,[4] H. Tydesjö,[20] N. Tyurin,[12] T. Ushiroda,[24] H. W. van Hecke,[19] C. Velissaris,[26] J. Velkovska,[28] M. Velkovsky,[28] A. A. Vinogradov,[16] M. A. Volkov,[16] A. Vorobyov,[30] E. Vznuzdaev,[30] H. Wang,[5] Y. Watanabe,[31,32] S. N. White,[3] C. Witzig,[3] F. K. Wohn,[13] C. L. Woody,[3] W. Xie,[5,42] K. Yagi,[39] S. Yokkaichi,[31] G. R. Young,[29] I. E. Yushmanov,[16] W. A. Zajc,[8] Z. Zhang,[28] and S. Zhou[6]

(PHENIX Collaboration)

[1]*Institute of Physics, Academia Sinica, Taipei 11529, Taiwan*
[2]*Bhabha Atomic Research Centre, Bombay 400 085, India*
[3]*Brookhaven National Laboratory, Upton, New York 11973-5000*
[4]*Department of Physics, Banaras Hindu University, Varanasi 221005, India*
[5]*University of California–Riverside, Riverside, California 92521*
[6]*China Institute of Atomic Energy (CIAE), Beijing, People's Republic of China*
[7]*Center for Nuclear Study, Graduate School of Science, University of Tokyo, 7-3-1 Hongo, Bunkyo, Tokyo 113-0033, Japan*

[8]Columbia University, New York, New York 10027
and Nevis Laboratories, Irvington, New York 10533
[9]Florida State University, Tallahassee, Florida 32306
[10]Georgia State University, Atlanta, Georgia 30303
[11]Hiroshima University, Kagamiyama, Higashi-Hiroshima 739-8526, Japan
[12]Institute for High Energy Physics (IHEP), Protvino, Russia
[13]Iowa State University, Ames, Iowa 50011
[14]KEK, High Energy Accelerator Research Organization, Tsukuba-shi, Ibaraki-ken 305-0801, Japan
[15]Korea University, Seoul, 136-701, Korea
[16]Russian Research Center "Kurchatov Institute," Moscow, Russia
[17]Kyoto University, Kyoto 606, Japan
[18]Lawrence Livermore National Laboratory, Livermore, California 94550
[19]Los Alamos National Laboratory, Los Alamos, New Mexico 87545
[20]Department of Physics, Lund University, Box 118, SE-221 00 Lund, Sweden
[21]McGill University, Montreal, Quebec, Canada H3A 2T8
[22]Institut für Kernphysik, University of Münster, D-48149 Münster, Germany
[23]Myongji University, Yongin, Kyonggido 449-728, Korea
[24]Nagasaki Institute of Applied Science, Nagasaki-shi, Nagasaki, 851-0193, Japan
[25]University of New Mexico, Albuquerque, New Mexico 87131
[26]New Mexico State University, Las Cruces, New Mexico 88003
[27]Chemistry Department, State University of New York–Stony Brook, Stony Brook, New York 11794
[28]Department of Physics and Astronomy, State University of New York–Stony Brook, Stony Brook, New York 11794
[29]Oak Ridge National Laboratory, Oak Ridge, Tennessee 37831
[30]PNPI, Petersburg Nuclear Physics Institute, Gatchina, Russia
[31]RIKEN (The Institute of Physical and Chemical Research), Wako, Saitama 351-0198, Japan
[32]RIKEN BNL Research Center, Brookhaven National Laboratory, Upton, New York 11973-5000
[33]Universidade de São Paulo, Instituto de Física, Caixa Postal 66318, São Paulo CEP05315-970, Brazil
[34]SUBATECH (Ecole des Mines de Nantes, IN2P3/CNRS, Universite de Nantes), BP 20722-44307, Nantes-Cedex 3, France
[35]St. Petersburg State Technical University, St. Petersburg, Russia
[36]University of Tennessee, Knoxville, Tennessee 37996
[37]Department of Physics, Tokyo Institute of Technology, Tokyo, 152-8551, Japan
[38]University of Tokyo, Tokyo, Japan
[39]Institute of Physics, University of Tsukuba, Tsukuba, Ibaraki 305, Japan
[40]Vanderbilt University, Nashville, Tennessee 37235
[41]Waseda University, Advanced Research Institute for Science and Engineering, 17 Kikui-cho, Shinjuku-ku, Tokyo 162-0044, Japan
[42]Weizmann Institute, Rehovot 76100, Israel
[43]Yonsei University, IPAP, Seoul 120-749, Korea
[44]KFKI Research Institute for Particle and Nuclear Physics (RMKI), Budapest, Hungary[†]
(Received 16 January 2002; published 30 April 2002)

Two-pion correlations in $\sqrt{s_{NN}} = 130$ GeV Au + Au collisions at RHIC have been measured over a broad range of pair transverse momentum k_T by the PHENIX experiment at RHIC. The k_T dependent transverse radii are similar to results from heavy-ion collisions at $\sqrt{s_{NN}} = 4.1$, 4.9, and 17.3 GeV, whereas the longitudinal radius increases monotonically with beam energy. The ratio of the outwards to sidewards transverse radii ($R_{\mathrm{out}}/R_{\mathrm{side}}$) is consistent with unity and independent of k_T.

DOI: 10.1103/PhysRevLett.88.192302 PACS numbers: 25.75.Dw

The influence of Bose-Einstein statistics on the correlation of identical charged pions at low relative momentum was first used to probe the space-time structure of pion emission in $p\bar{p}$ annihilations [1] and has subsequently been applied to relativistic heavy-ion collisions from the Bevalac to RHIC [2–7] (see [8] for recent reviews) and to a wide range of systems including e^+e^- annihilations [9]. The correlation function is defined as the ratio of the two-particle probability distribution to the product of the single-particle distributions. For a static source with no final state interactions, it is related to the Fourier transform with respect to $\mathbf{q} = \mathbf{p}_1 - \mathbf{p}_2$ of the source distribution $\rho(\mathbf{r})$, $P(\mathbf{p}_1, \mathbf{p}_2)/P(\mathbf{p}_1)P(\mathbf{p}_2) = 1 + |\tilde{\rho}(\mathbf{q})|^2$ [1]. If the source is parametrized as a multidimensional Gaussian, the enhancement in the correlation function is a Gaussian, and the Gaussian widths are each inversely proportional to the source dimensions in the canonically conjugate spatial variables. The extracted source dimensions are commonly referred to as HBT radii, after a similar technique developed by Hanbury-Brown and Twiss to measure stellar radii [10]. For dynamic sources, such as rapidly expanding sources in heavy-ion collisions, the correlation function measures "lengths of homogeneity," or the relative separations of the pions with low relative momentum. This leads to source radii which depend strongly on k_T, the mean transverse momentum of the pion pair [11–16]. If the dynamics are correctly modeled, then both the source geometry and rate of expansion can be deduced by measuring the k_T dependence of the radii. The existence of a connection between HBT radii and heavy-ion source geometry is established by the dependence of the radii on system size [17], centrality [4,5], and reaction plane [3]. Interest in Bose-Einstein correlations in heavy-ion collisions is driven by the expectation that HBT radii are sensitive to the large and/or long-lived sources which may accompany a QCD phase transition [12,18]. Recent calculations predict that the greatest sensitivity to a long-lived source will come from measurements of the correlation function at high k_T (≥ 0.3 GeV/c) [19,20].

We present new measurements from the PHENIX experiment on two-pion correlations in Au + Au collisions at $\sqrt{s_{NN}} = 130$ GeV in the region $|\eta| < 0.35$, $0.2 < k_T < 1.0$ GeV/c, significantly extending previous measurements by STAR [7] up to a mean-k_T 0.63 GeV/c. The data are compared to theoretical predictions for RHIC and to HBT radii from lower energy collisions at the CERN Super Proton Synchrotron and Alternating Gradient Synchrotron (at BNL). The k_T dependence of the transverse radii is used to extract a geometric transverse radius.

The PHENIX experiment has been described in detail elsewhere [21,22]. For this analysis we utilize a subset of the detectors in PHENIX. We use the hadronic particle identification capabilities present in the west arm of the PHENIX spectrometer perpendicular to the beam direction [22] with polar and azimuthal ranges of $|\eta| < 0.35$ and $\pi/4$, respectively, during its first year of running. In this analysis, the vertex is determined with a zero degree calorimeter and a pair of Čerenkov beam-beam counters (BBC). Pattern recognition and momentum reconstruction rely on a drift chamber and a pad chamber which occupy the region between 2.0 and 2.5 m from the beam axis. The momentum resolution from these detectors is $\delta p/p = 0.6\% \oplus 3.6\% p$. Particle velocity is determined from the differential time measurements of the BBC and the electromagnetic calorimeter (EMC) [23], with a combined rms resolution of 700 ps, coupled with the path length determined from pattern recognition. The momentum determination and particle identification method are similar to [24], except that the time of flight is measured by the EMC. A pion is defined as being within 1.5 standard deviations of the pion mass-squared peak but at least 2.5 standard deviations away from the kaon peak. After applying interdetector association cuts the background from misassociated EMC hits is ~10% as determined by a hit randomization technique. This background does not significantly distort the extracted radius in the correlation measurements, although it reduces the measured correlation strength (λ). We did not correct for this background in our correlation analysis.

A total of 493 K events in the most central 30% of the cross section survive all off-line cuts. This sample contains 3.1 million π^+ pairs and 3.3 million π^- pairs in the analysis, and has a mean centrality of 10%.

The pion correlation function is determined from pairs of identical pions. The normalized probability of detecting two particles with relative momentum $\mathbf{q} = \mathbf{p}_1 - \mathbf{p}_2$ and average momentum $\mathbf{k} = (\mathbf{p}_1 + \mathbf{p}_2)/2$ is determined experimentally by the ratio of pairs from the same event (A) with those from different events (B): $C_2(\mathbf{q}, \mathbf{k}) = A(\mathbf{q}, \mathbf{k})/B(\mathbf{q}, \mathbf{k})$. Pairs of particles within 2 cm of each other in the drift chamber are eliminated from the analysis in both the real and background samples. Pairs that share the same EMC cluster are also removed from both samples. Finally, all pairs in the mixed background sample are required to be from events with a reconstructed BBC collision vertex within 1 cm of each other.

We correct for the Coulomb interaction of the pairs in the correlation function by parametrizing the source as a Gaussian distribution in the pair center-of-mass frame and performing an iterative procedure [25] which accounts for the finite resolution of the detector. This procedure applied to the distribution of π^+-π^- pairs is in agreement with the data, although the statistics in the Run-1 opposite-signed analysis are not sufficient to independently determine the required Coulomb correction. Systematic studies of the Coulomb correction which vary both radius and magnitude within reasonable constraints produce variations in the final radii which never exceed 0.25 fm.

The relative momenta are projected into the variables $q_{\rm long}$, along the beam direction, $q_{\rm out}$, parallel to the transverse momentum of the pair $\mathbf{k}_T = \frac{1}{2}(\mathbf{p}_{T_1} + \mathbf{p}_{T_2})$, and $q_{\rm side}$, perpendicular to $q_{\rm long}$ and $q_{\rm out}$ [11,18]. These variables are calculated in the longitudinal comoving system (LCMS), obtained by a longitudinal boost from the lab frame to the frame in which the longitudinal pair velocity vanishes. This frame is commonly used for sources expected to be invariant under longitudinal boosts [26].

The fully corrected correlation function for π^- pairs is shown in the top panels of Fig. 1; the large q region of the correlation function has been normalized to 1 in the plots. The data are fit to a Gaussian parametrization of the source using a MINUIT based log-likelihood method [4].

$$C_2 = 1 + \lambda \exp(-R_{\rm long}^2 q_{\rm long}^2 - R_{\rm side}^2 q_{\rm side}^2 - R_{\rm out}^2 q_{\rm out}^2), \quad (1)$$

where $R_{\rm long}$, $R_{\rm side}$, and $R_{\rm out}$ are the conjugate variables to $q_{\rm long}$, $q_{\rm side}$, and $q_{\rm out}$, respectively. Errors quoted in the tables and figures are statistical only. Systematic errors come mainly from the Coulomb correction and dependence of the results on the two-track distance cuts. The combined systematic error for these effects, estimated by varying the cuts and corrections within reasonable bounds, is 8% for $R_{\rm long}$, and $R_{\rm side}$, and 4% for $R_{\rm out}$. The systematic error from residual correlations in the event-mixed background [2] is 2%, yielding a total systematic error of ~8% for $R_{\rm long}$ and $R_{\rm side}$ and ~4.5% for $R_{\rm out}$.

The data set is subdivided into three k_T bins of equivalent statistics in order to study the momentum dependence of the correlation function. In Fig. 2, the radii for π^-

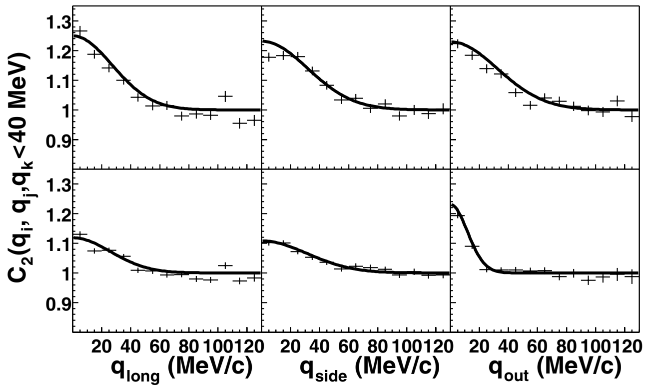

FIG. 1. The three dimensional correlation function for π^- pairs versus $q_{\rm long}$, $q_{\rm side}$, and $q_{\rm out}$ in both the LCMS frame (top) and the pair center-of-mass frame (bottom). The data are plotted versus one momentum difference variable while requiring the other two to be less than 40 MeV$/c$. The lines correspond to the fit to the entire distribution.

pairs are shown to agree within statistical and systematic errors with previous measurements for overlapping k_T bins at this energy for the 12% most central events. For STAR, the mean pair centrality can be approximated by the geometric mean of 8%, which is slightly more central than the mean pair centrality of 10% for the PHENIX data. This figure also shows k_T dependent radii for midrapidity pions from central collisions for $\sqrt{s_{NN}} = 17.3$ GeV Pb + Pb [6,27] and for $\sqrt{s_{NN}} = 4.9$ and 4.1 GeV Au + Au [3,4]. For the transverse radii, $R_{\rm out}$ and $R_{\rm side}$, the variation with collision energy is generally smaller than the statistical and systematic errors of the individual data points. There is no evidence for a change in the low-k_T extrapolation of $R_{\rm side}$ with increasing $\sqrt{s_{NN}}$ which would indicate a larger geometric source at higher energy. Nor is any change evident in $R_{\rm out}$ relative to $R_{\rm side}$ at high k_T, indicating a longer-lived source. This result is surprising given the factor of $\sim$3 change in the total charged particle multiplicity per unit rapidity at midrapidity [28]. Only $R_{\rm long}$ exhibits a significant variation with collision energy. To quantify this difference, we fit the $R_{\rm long}$ dependence to $A/\sqrt{m_T}$ [13,16,29] for the three sets of beam energies. The results are overlayed with the data in the bottom panel of Fig. 2 and yield $A = 3.32 \pm 0.03$, 3.05 ± 0.06, and 2.19 ± 0.05 fm GeV$^{1/2}$ for $\sqrt{s_{NN}} = 130$, 17.3, and 4.9/4.1 GeV, respectively.

Although a finite emission duration contributes to $R_{\rm out}$ but not to $R_{\rm side}$, dynamical correlations affect the two radii differently. A quantitative determination of the source lifetime can be performed only in the context of a dynamical model. The lower panel of Fig. 3 shows the k_T dependence

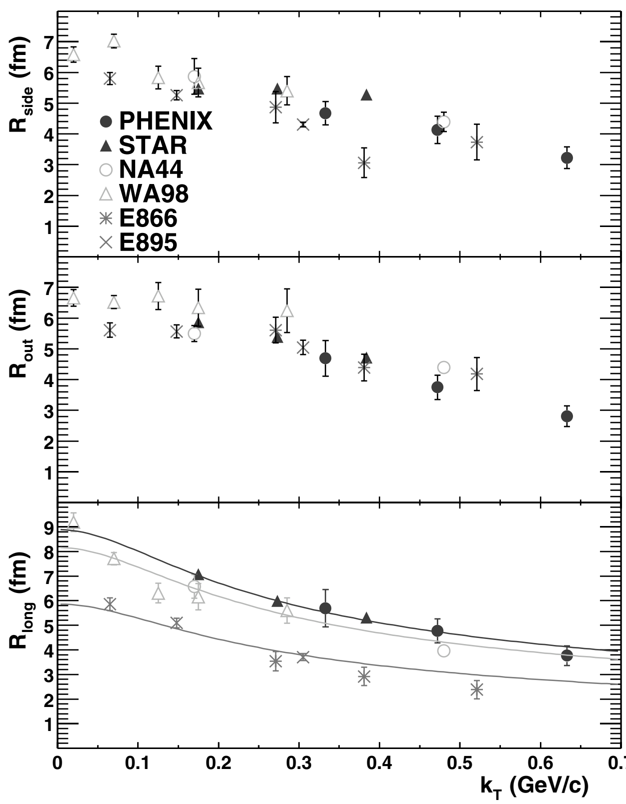

FIG. 2. HBT radii for pion pairs as a function of k_T measured at midrapidity for various energies from E895 ($\sqrt{s_{NN}} = 4.1$ GeV), E866 ($\sqrt{s_{NN}} = 4.9$ GeV), NA44, WA98 ($\sqrt{s_{NN}} = 17.3$ GeV), STAR, and PHENIX Collaborations ($\sqrt{s_{NN}} = 130$ GeV). The bottom plot includes fits to $A/\sqrt{m_T}$ for each energy region. The data are for π^- results except for the NA44 results, which are for π^+.

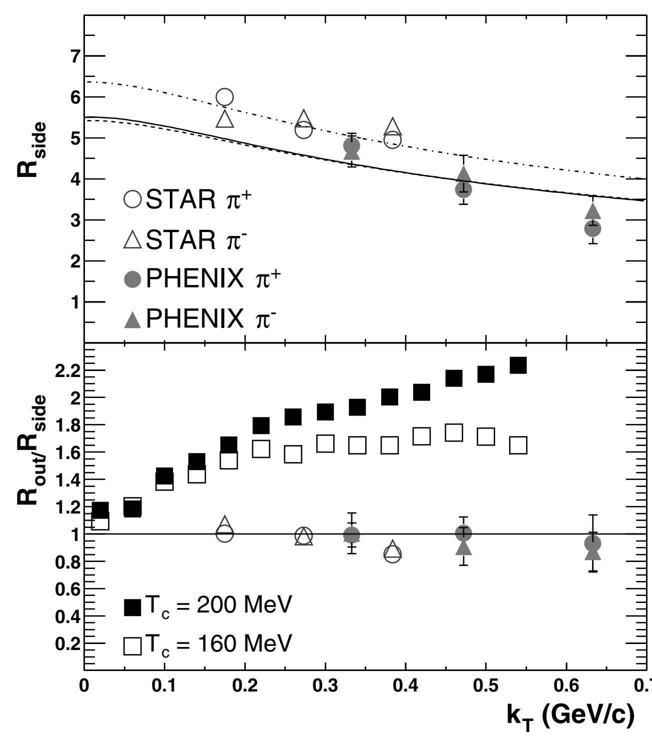

FIG. 3. The top panel shows the measured $R_{\rm side}$ from identical pions for STAR and PHENIX. The solid line is a fit of Eq. (3) to the PHENIX data, and the dashed line is the same fit for Eq. (2). The dot-dashed line is a fit of Eq. (3) to the STAR data. The bottom panel shows the ratio $R_{\rm out}/R_{\rm side}$ as a function of k_T overlayed with theoretical predictions for a phase transition for two critical temperatures.

TABLE I. The k_T dependencies of the π^+ and π^- radii in the LCMS and PCMS frames. All momenta are in MeV and all radii are in fm. The errors are statistical only.

	k_T (MeV)	200–400	400–550	550–1000
	$\langle k_T \rangle$	333	472	633
π^+	$R_{\rm inv}$	6.74 ± 0.31	6.42 ± 0.46	3.46 ± 0.46
	$\lambda_{\rm LCMS}$	0.423 ± 0.037	0.389 ± 0.039	0.287 ± 0.048
	$R_{\rm long}$	6.01 ± 0.45	4.76 ± 0.35	2.97 ± 0.38
	$R_{\rm side}$	4.81 ± 0.30	3.74 ± 0.36	2.79 ± 0.37
	$R_{\rm out}$	4.78 ± 0.30	3.76 ± 0.26	2.59 ± 0.46
	$R_{\rm out}^{\rm PCMS}$	11.35 ± 0.69	12.20 ± 1.02	8.60 ± 1.13
π^-	$R_{\rm inv}$	6.00 ± 0.30	5.96 ± 0.41	4.58 ± 0.48
	$\lambda_{\rm LCMS}$	0.431 ± 0.079	0.405 ± 0.067	0.353 ± 0.062
	$R_{\rm long}$	5.69 ± 0.76	4.77 ± 0.49	3.76 ± 0.41
	$R_{\rm side}$	4.67 ± 0.38	4.13 ± 0.45	3.22 ± 0.35
	$R_{\rm out}$	4.69 ± 0.58	3.75 ± 0.40	2.81 ± 0.34
	$R_{\rm out}^{\rm PCMS}$	11.27 ± 0.72	12.42 ± 1.18	11.89 ± 1.73

of the ratio $R_{\rm out}/R_{\rm side}$ for PHENIX and STAR along with recent calculations for a thermalized source which undergoes a first order phase transition at critical temperatures (T_c) of 160 and 200 MeV [20]. The rise in $R_{\rm out}/R_{\rm side}$ which comes predominantly from a hadronic rescattering phase is not present in the data, and the values of 1.6 ($T_c = 160$ MeV) and 2.2 ($T_c = 200$ MeV) at high k_T are excluded.

An additional consequence of strong dynamics occurs for sources in which the transverse expansion is relativistic. In this case, $R_{\rm out}$ measured in the LCMS frame is Lorentz contracted by the γ of the pion source velocity along the direction of $q_{\rm out}$ [30,31]. Current Lorentz invariant formulations of the correlation function [14,32] are insufficient to determine the source velocity due to transverse expansion; however, the pair center-of-mass system (PCMS) can be used to provide an upper limit on $R_{\rm out}$ [33]. The correlation function for π^- pairs in the PCMS frame is shown in the bottom panels of Fig. 1, and fit results for $R_{\rm out}^{\rm PCMS}$ are listed in Table I. As expected, $R_{\rm side}$ and $R_{\rm long}$ are equal to the corresponding LCMS parameters within errors.

Two analytic expressions have been used to describe $R_{\rm side}$ as a function of $m_T = \sqrt{k_T^2 + m_\pi^2}$ for a transversely expanding source,

$$R_{\rm side}^2(m_T) = \frac{R_{\rm geom}^2}{1 + \beta_f^2(\frac{m_T}{T})}, \quad (2)$$

$$R_{\rm side}^2(m_T) = \frac{R_{\rm geom}^2}{1 + \eta_f^2(\frac{1}{2} + \frac{m_T}{T})}. \quad (3)$$

Equation (2) is a first order approximation in $\frac{T}{m_T}$ for a longitudinally boost invariant source with finite temperature, T, and expansion velocity, $\beta_T = \beta_f \rho / R_{\rm geom}$, where $R_{\rm geom}$ is the Gaussian transverse radius [14]. Equation (3) includes an additional term in the approximation and the linear transverse expansion velocity is replaced by a transverse rapidity, $\eta_T = \eta_f \rho / R_{\rm geom}$ [16]. For a transverse surface rapidity of $\eta_f = 0.85$ ($\beta_f = 0.69$) and $T = 125$ MeV [34], a fit of Eq. (3) to the PHENIX $R_{\rm side}$ m_T dependence yields $R_{\rm geom} = 8.1 \pm 0.3$ fm with a $\chi^2/{\rm d.o.f.} = 9.6/6$. To assess systematic errors the PHENIX data are also fit to Eq. (2), yielding $R_{\rm geom} = 6.7 \pm 0.2$ fm and $\chi^2/{\rm d.o.f.} = 9.1/6$, and the STAR data are fit to Eq. (3), yielding $R_{\rm geom} = 9.4 \pm 0.1$ fm with $\chi^2/{\rm d.o.f.} = 21/6$. These fits are shown in the top panel of Fig. 3. All values of $R_{\rm geom}$ are significantly larger than the comparable 1D rms radius for a Au nucleus [35] of $\sqrt{1/3} \times \sqrt{3/5} \times 6.87 = 3.07$ fm.

In conclusion, we have extended the measurement of two particle correlations for Au + Au collisions at $\sqrt{s_{NN}} = 130$ GeV to $\langle k_T \rangle = 0.63$ GeV/c using the PHENIX detector at RHIC. Values of $R_{\rm out}^{\rm PCMS}$ are used to constrain the Lorentz effects for a relativistic transverse expansion. Fitting $R_{\rm side}(k_T)$ to two analytic expressions for an expanding source yields a transverse geometric radius that is much larger than the comparable radius for Au. We find that $R_{\rm long}(k_T)$ increases monotonically with collision energy, yet no energy dependence is discernible in the k_T dependence of $R_{\rm out}$ and $R_{\rm side}$, and the ratio, $R_{\rm out}/R_{\rm side}$, is consistent with unity and independent of k_T. The results for the transverse radii are contrary to common expectations for a first order phase transition in Au + Au collisions at these energies, as demonstrated by the comparison to a typical hydrodynamic model with hadronic rescattering. Therefore, we conclude that current concepts regarding the space-time evolution of the pion source inferred from two-pion correlations in Au + Au collisions at RHIC will need to be revised.

We thank the staff of the Collider-Accelerator and Physics Departments at BNL for their vital contributions. We acknowledge support from the Department of Energy and NSF (U.S.A.), MEXT and JSPS (Japan), RAS, RMAE, and RMS (Russia), BMBF, DAAD, and AvH (Germany), VR and KAW (Sweden), MIST and NSERC (Canada), CNPq and FAPESP (Brazil), IN2P3/CNRS

(France), DAE and DST (India), KRF and CHEP (Korea), the U.S. CRDF for the FSU, and the U.S.–Israel BSF.

*Deceased.

†Not a participating Institution.

[1] G. Goldhaber *et al.,* Phys. Rev. **120**, 300 (1960).
[2] W. A. Zajc *et al.,* Phys. Rev. C **29**, 2173 (1984).
[3] M. Lisa *et al.,* Phys. Rev. Lett. **84**, 2798 (2000).
[4] E802 Collaboration, R. Soltz *et al.,* Nucl. Phys. **A661**, 439 (1999); L. Ahle *et al.,* nucl-ex/0204001.
[5] I. G. Bearden *et al.,* Eur. J. Phys. C **18**, 317 (2000).
[6] M. M. Aggarwal *et al.,* Eur. J. Phys. C **16**, 445 (2000).
[7] STAR Collaboration, C. Adler *et al.,* Phys. Rev. Lett. **87**, 082301 (2001).
[8] U. Wiedemann and U. Heinz, Phys. Rep. **319**, 145 (1999); T. Csörgő, Heavy Ion Phys. **15**, 1 (2002).
[9] G. Abbiendi *et al.,* Eur. J. Phys. C **16**, 423 (2000).
[10] R. Hanbury-Brown and R. Twiss, Philos. Mag. **45**, 663 (1954).
[11] S. Pratt, Phys. Rev. Lett. **53**, 1219 (1984).
[12] S. Pratt, Phys. Rev. D **33**, 1314 (1986).
[13] A. N. Makhlin and Y. M. Sinyukov, Z. Phys. C **39**, 69 (1988).
[14] S. Chapman, J. R. Nix, and U. Heinz, Phys. Rev. C **52**, 2694 (1995).
[15] D. E. Fields *et al.,* Phys. Rev. C **52**, 986 (1995).
[16] U. Wiedemann, P. Scotto, and U. Heinz, Phys. Rev. C **53**, 918 (1996).
[17] J. Bartke, Phys. Lett. B **174**, 32 (1986).
[18] G. Bertsch and G. E. Brown, Phys. Rev. C **40**, 1830 (1989).
[19] D. Rischke and M. Gyulassy, Nucl. Phys. **A608**, 479 (1996).
[20] S. Soff, S. A. Bass, and A. Dumitru, Phys. Rev. Lett. **86**, 3981 (2001).
[21] D. P. Morrison, Nucl. Phys. **A638**, 565c (1998); N. Saito, *ibid.* 575c (1998).
[22] PHENIX Collaboration, H. Hamagaki *et al.,* Nucl. Phys. **A698**, 412C (2002).
[23] PHENIX Collaboration, S. White *et al.,* Nucl. Phys. **A698**, 420C (2002).
[24] K. Adcox *et al.,* nucl-ex/0112006.
[25] M. D. Baker, Nucl. Phys. **A610**, 213c (1996).
[26] J. D. Bjorken, Phys. Rev. D **27**, 140 (1983); F. Cooper, G. Frye, and E. Schonberg, Phys. Rev. D **11**, 192 (1975).
[27] NA44 Collaboration, I. G. Bearden *et al.,* Phys. Rev. C **58**, 1656 (1998).
[28] L. Ahle *et al.,* Phys. Rev. C **57**, R466 (1998); D. B. Back *et al.,* Phys. Rev. Lett. **85**, 3100 (2000).
[29] This functional form is motivated by an approximation in T/m_T in which $A = \tau_0 T$, where τ_0 is the proper time of hadronization.
[30] S. Pratt, T. Csörgo, and J. Zimanyi, Phys. Rev. C **42**, 2646 (1990).
[31] *Particle Production in Highly Excited Matter,* edited by H. H. Gutbrod and J. Rafelski (Plenum Press, New York, 1993), p. 435.
[32] F. Yano and S. Koonin, Phys. Lett. **78B**, 556 (1978).
[33] Here the radii are Lorentz *extended* by γ_s measured in the PCMS frame. For a toy model of an azimuthally symmetric source in motion but not expanding, $R_{\rm out}^{\rm PCMS} = \gamma_s \sqrt{R_{\rm side}^2 + \beta_s^2 \tau^2}$.
[34] These values are taken from fits to the single particle spectra for the 5%−15% centrality bin for a linear velocity profile in a hard sphere. For a linear transverse rapidity in a Gaussian source these values vary by less than 2%.
[35] B. Hahn, D. G. Ravenhall, and R. Hofstadter, Phys. Rev. **101**, 1131 (1956).